



OPEN ACCESS

EDITED BY

Santanu Bhattacharya,
Mayo Clinic Florida, United States.

REVIEWED BY

Kaushlendra Tripathi,
University of Alabama at Birmingham,
United States
JIA LI,
University of North Carolina at Charlotte,
United States.

*CORRESPONDENCE

Aleksandra Gawrylak,
✉ agawrylak@wim.mil.pl

RECEIVED 11 February 2025

ACCEPTED 09 April 2025

PUBLISHED 13 June 2025

CITATION

Gawrylak A, Brodaczewska K,
Iwanicka-Nowicka R, Kobłowska M,
Synowiec A, Bodnar L, Szczylik C, Lesyng B,
Stec R and Kieda C (2025) Hypoxia alters the
response of ovarian cancer cells to the
mitomycin C drug.
Front. Cell Dev. Biol. 13:1575134.
doi: 10.3389/fcell.2025.1575134

COPYRIGHT

© 2025 Gawrylak, Brodaczewska,
Iwanicka-Nowicka, Kobłowska, Synowiec,
Bodnar, Szczylik, Lesyng, Stec and Kieda. This
is an open-access article distributed under
the terms of the [Creative Commons
Attribution License \(CC BY\)](#). The use,
distribution or reproduction in other forums is
permitted, provided the original author(s) and
the copyright owner(s) are credited and that
the original publication in this journal is cited,
in accordance with accepted academic
practice. No use, distribution or reproduction
is permitted which does not comply with
these terms.

Hypoxia alters the response of ovarian cancer cells to the mitomycin C drug

Aleksandra Gawrylak ^{1,2*}, Klaudia Brodaczewska ¹,
Roksana Iwanicka-Nowicka ^{3,4}, Marta Kobłowska ^{3,4},
Agnieszka Synowiec ¹, Lubomir Bodnar ^{5,6},
Cezary Szczylik ⁷, Bogdan Lesyng ⁸, Rafał Stec ⁹ and
Claudine Kieda ^{1,10}

¹Military Institute of Medicine – National Research Institute, Laboratory of Molecular Oncology and Innovative Therapies, Szaserów, Warsaw, Poland, ²Department of Immunology, Institute of Functional Biology and Ecology, Faculty of Biology, University of Warsaw, Warsaw, Poland, ³Laboratory of Systems Biology, Faculty of Biology, University of Warsaw, Warsaw, Poland, ⁴Laboratory of Microarray Analysis, Institute of Biochemistry and Biophysics, Polish Academy of Sciences, Warsaw, Poland, ⁵Faculty of Medical and Health Sciences, Siedlce University of Natural Sciences and Humanities, Siedlce, Poland, ⁶Department of Clinical Oncology and Radiotherapy, St. John Paul II Mazovia Regional Hospital in Siedlce, Siedlce, Poland, ⁷Department of Oncology, Centre of Postgraduate Medical Education, European Health Centre, Otwock, Poland, ⁸Division of Biophysics and Center for Machine Learning, Faculty of Physics, University of Warsaw, Warsaw, Poland, ⁹Oncology Department, Medical University of Warsaw, Warsaw, Poland, ¹⁰Center for Molecular Biophysics UPR 4301 CNRS, Orleans, France

Introduction: Discrepancies between preclinical tests and clinical results raise serious concerns about the appropriateness of the current methodologies. In particular, cell biology approaches neglect fundamental physical parameters despite their relevance to *in vivo* conditions. Oxygen availability is critical for cell reactions; thus, the lack of consideration of hypoxia as the main regulator of the tumor microenvironment (TME) leads to misinterpreted data with consequences for translational applications. In this study, we show that mitomycin C (MMC), an antineoplastic antibiotic, is rarely used in ovarian cancer (OC) treatment despite its potential efficacy; we use MMC as an example of a treatment that warrants reevaluation under microenvironmental conditions, particularly during *in vitro* testing.

Methods: To evaluate the effects of MMC and oxygen tension (pO₂) on OC cells (SKOV3), HTA 2.0 microarrays were used, which demonstrated that hypoxia and MMC induced transcriptomic changes in OC cells. Their combination particularly emphasized the effect of pO₂ modification on MMC activity. The most significant findings were verified in three other OC cell lines, namely, TOV112D, ES-2, and A2780.

Results: Under normoxic conditions, MMC mostly affected several pathways associated with ribosome-related processes, whereas under hypoxic conditions, it induced modifications in the extracellular matrix (ECM). The most significantly upregulated gene in response to hypoxia–MMC treatment was *MMP1*, regulated by both MMC and hypoxia. Low pO₂ levels during MMC treatment allowed the identification of important regulators, such as *SPP1*, and the corresponding processes, including cholesterol biosynthesis.

Conclusion: Hypoxia modulated the effects of MMC on OC cells and identified genes that may serve as promising targets to enhance the effectiveness of MMC treatment.

KEYWORDS

ovarian cancer, hypoxia, mitomycin c, transcriptome, differential gene expression, pathway analysis

Introduction

Epithelial ovarian cancer (EOC), a global problem and challenge for modern oncology, affects vast numbers of women worldwide; in 2022, 324,398 new cases were recorded, reducing the life quality and length and causing numerous deaths (206,839) (Bray et al., 2024). Epidemiologically, the general downward trend in ovarian cancer (OC) morbidity results from progress in diagnostics and new targeted therapies. However, EOC still ranks eighth in terms of incidence and is the fifth most common cause of cancer-related death in women (Sung et al., 2021), thus being the most lethal tumor in the female reproductive system (Buklaho et al., 2023).

Predominant risk factors, such as hereditary mutations in genes predisposing to cancer development, account for 20%–25% of EOC cases (Bellcross, 2022). For years, OC treatment was based on a cytoreductive surgery and chemotherapy combination. The most active drugs for newly diagnosed advanced OC are platinum analogs and taxanes (Bogani et al., 2017; Pignata et al., 2019). Despite complete remission after such initial treatment, most patients (65%–80%) experience relapses within the first 5 years. The platinum-free interval is a predictor of treatment effectiveness (Duan et al., 2023). Maintenance therapy with PARP inhibitors and bevacizumab in the first, second, and subsequent lines of treatment is a recent progress in OC therapy (Sznurkowski, 2023).

In platinum-sensitive relapses, platinum salts remain the mainstay of treatment, while in platinum-resistant cases, progressing within 6 months (Colombo et al., 2019), no effective treatment exists. Mitomycin C (MMC), an alkylating cytostatic agent, was one of the drugs tested in platinum-resistant OC, showing a moderate 12% response (Hoskins et al., 1990). The response may be due to the inactivation of homologous recombination (HR) genes (Botrus et al., 2022). In tumors with functional repair deficiencies in HR, MMC may increase the activity of PARP inhibitors (veliparib) (Villalona-Calero et al., 2016). Chen X et al. showed that MMC may be particularly active in cancers with monoallelic and biallelic BRCA2 mutant genes. MMC significantly reduced BRCA2 mRNA and protein expression in BRCA2-mutated cell lines but not in wild-type BRCA2 cell lines, suggesting that BRCA2 inactivation is crucial for the MMC therapeutic effect (Chen et al., 2020).

Hence, the use of MMC in OC patients with HR disorders has gained attention. Promising effects were obtained in clinical trials of neoadjuvant treatment of OC combining MMC with

cisplatin (Gorodnova et al., 2018) or in a three-drug regimen with doxorubicin (Gorodnova et al., 2021). MMC with cisplatin is also promising in treating recurrent OC caused by *BRCA1* gene mutations (Gorodnova et al., 2020). *BRCA1* expression is dependent on oxygen tension (pO_2) (Bindra et al., 2005; Lu et al., 2011; Fanale et al., 2013), with a strong impact on tumor suppressor factor activity (Li et al., 2018). OCs are highly hypoxia-dependent (Shih et al., 2021); thus, there is a need to study the drug performance under biologically representative conditions. Hypoxia—defined as the partial pressure of oxygen below the physiological levels—affects many cellular processes, including angiogenesis, epithelial-to-mesenchymal transition (EMT), and the acquisition of stem-like properties of aggressive cancer cells (Collet et al., 2012; Chouaib et al., 2018). Low oxygen tension stabilizes the hypoxia-inducible factor 1 α (HIF-1 α), and hypoxia reduces the effectiveness of drugs used to treat OC (Evans et al., 2012; Klemba et al., 2020).

Although MMC is used to treat several types of cancer (Lister-Sharp et al., 2000; Stec et al., 2014), knowledge about its effects on OC cells is limited (Strese et al., 2013). To date, its effects have not been studied under appropriate biologically relevant conditions, including hypoxia. To decipher its real effect in such conditions, a systemic approach was chosen using transcriptomic analysis to identify genes involved in the response of OC SKOV3 cells to MMC under hypoxic tumor-like conditions, and the most significant findings were verified in three other OC cell lines. Thus, this study aims to evaluate the effects of hypoxia, MMC, and their combination on SKOV3 cancer cells, with emphasis on transcriptomic analysis and the differential expression of genes.

Materials and methods

Cells and treatment procedure

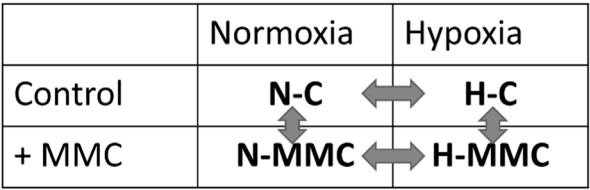
Human OC cells SKOV3 (ATCC, Cat#HTB-77) were cultured in RPMI-1640 GlutaMAXTM medium supplemented with 10% fetal bovine serum (FBS) (Thermo Fisher Scientific, United States; RPMI: Cat#61870036 and FBS: Cat#A5209401) for microarray experiments. SKOV3, TOV112D (ATCC, Cat#CRL-11731), ES-2 (ATCC, Cat#CRL-1978), and A2780 (ECACC, Cat#93112519) were maintained in Opti-MEM with 2% FBS (Thermo Fisher Scientific, United States; Opti-MEM: Cat#31985070 and FBS: Cat#A5209401) for other analyses. Mycoplasma-free (PromoKine, Cat#PK-CA91-1096) cells were passaged ($p < 10$) at 80% confluence using Accutase (BioLegend, United States, Cat#423201) for detachment.

SKOV3 cells seeded in a T-25 flask with 5 mL of medium were incubated for 24 h under normoxic conditions. After 24 h, the medium was replaced with preconditioned medium (incubated

Abbreviations: DEG, differentially expressed gene; ECM, extracellular matrix; GO, Gene Ontology; IPA, Ingenuity Pathway Analysis; KEGG, Kyoto Encyclopedia of Genes and Genomes; MMC, mitomycin C; OC, ovarian cancer; pO_2 , oxygen tension; TME, tumor microenvironment.

under normoxic and hypoxic conditions for 24 h before the experiment), with or without 1.16 μM of MMC (Sigma-Aldrich, Cat#M4287), and the flasks were incubated for the following 72 h before collecting materials (cells, protein, and RNA) for further analyses (FACS, WB, qPCR, ELISA, and microarrays). Cell numbers were assessed using the Trypan Blue exclusion test (Thermo Fisher Scientific, Cat#15250061) in a Burkner chamber. Hypoxic conditions were achieved using an atmosphere of N_2 94%/CO₂ 5%/O₂ 1% (BioSpherix, Xvivo System Model X3).

The experimental setup combining the pO₂ levels and MMC treatment is schematically presented in the following sections, resulting in four distinct experimental groups, namely, normoxia control (without treatment; N-C), normoxia with MMC treatment (N-MMC), hypoxia control (without treatment; H-C), and hypoxia with MMC treatment (H-MMC).



Detailed descriptions of the cell treatments used in the experiments reported in Supplementary Figures are provided in Supplementary Materials and Methods.

Cell size, granularity, and cell cycle analysis

SKOV3 cells (2.25×10^5 cells) seeded in T25 flasks and maintained under normoxia conditions were treated with MMC as mentioned above. Cell size and granularity were assessed by flow cytometry (FACSCalibur, Becton Dickinson, United States), using forward-scatter (FSC) and side-scatter (SSC) parameters, and data were analyzed using FCS Express 7 software (*De Novo Software*). Cell cycle analysis was performed by flow cytometry after 72 h of treatment; cells were fixed overnight at 4°C in 70% ethanol and stained with propidium iodide (BD Pharmingen™ PI Staining Solution, Becton Dickinson) to determine DNA content. Cell proportions in G0/G1, S, and G2/M phases were calculated using FCS Express 7 software (*De Novo Software*). A total of 10^4 events were analyzed per sample.

Evaluation of the Ki67+ population

The proportion of actively proliferating Ki67+ cells was investigated. Nuclear Ki67 is expressed in G1, S, G2, and M phases but absent in the G0 phase. Permeabilized cells were stained with a phycoerythrin-labeled (PE) anti-human Ki67 IgG1 antibody (Merck Millipore, United States, Cat#MCH100114) and analyzed by flow cytometry (BD FACSCalibur). IgG1-PE-stained cells served as the negative control. A total of 10^4 events were analyzed per sample.

LDH activity measurement

MMC cytotoxicity toward SKOV3 cells under normoxia vs hypoxia was assessed by measuring lactate dehydrogenase (LDH)

activity in the SKOV3 cell culture supernatants after a 72-h treatment with (or without) MMC (LDH-Cytox Assay Kit, BioLegend, Cat#326401), and the orange formazan product was measured by absorbance at 490 nm using a microplate reader (Multiskan GO, Thermo Fisher Scientific Oy, Ratastie, Finland). Results are presented as relative toxicity.

RNA isolation

Total RNA was extracted from the SKOV3 cells incubated with or without MMC under normoxia or hypoxia using a Direct-zol RNA Miniprep Kit (Zymo Research, Irvine, CA, United States, Cat#R2050). Genomic DNA was removed using a TURBO DNA-free Kit (Thermo Fisher Scientific, United States, Cat#AM 1907). RNA quality and concentration were determined by absorbance measurement at 230 nm, 260 nm, and 280 nm using the μDrop plate in a microplate reader (Thermo Fisher Scientific, Finland). RNA samples meeting the criteria of a 260/230 ratio >2 and a 260/280 ratio within 1.8–2.0 was used for further analysis.

Microarray analysis

Total RNA isolated from SKOV3 cells was analyzed using Human Transcriptome Array (HTA) 2.0 (Affymetrix, Santa Clara, CA, United States, Cat#902162). RNA quality control (RNA integrity number, RIN) was assessed using the Bioanalyzer 2100 (Agilent Technologies, Waldbronn, Germany). HTA 2.0 arrays were performed as described by Koczan et al. (2018) and scanned using the GeneChip Scanner 3000 7G (Affymetrix).

HTA 2.0 microarray scans were visually inspected using Affymetrix GeneChip Command Console (AGCC), generating CEL files with processed pixel intensity values for each probe. The CEL files (N = 16, 1 GB of data) were imported to Transcriptome Analysis Console 4.0.2 software (TAC 4.0.2, Affymetrix) to summarize the probe set using the robust multi-array average (RMA) algorithm, including background correction, quantile normalization, and a log2 transformation of data, which was later used in the gene-level analysis. Each HTA 2.0 microarray contains data on 67,528 genes, 28,6263 full-length transcripts, and 67,0402 exons (including coding and non-coding transcripts).

Transcriptomic data analysis

Differentially expressed genes (DEGs) were identified using TAC 4.0.2 software (Affymetrix, Santa Clara, CA, United States) and the ANOVA method for statistical testing with ebayes (Empirical Bayes Statistics for Differential Expression) correction for a small sample size. The DEG analysis was performed on the DEGs meeting the criteria of gene-level fold change < -2 or >2 and $p < 0.05$.

Venn diagram was prepared in InteractiVenn (Heberle et al., 2015) (<https://www.interactivenn.net/>). Gene Ontology (GO) and Kyoto Encyclopedia of Genes and Genomes (KEGG) pathway functional analyses were performed using SRplot software (<https://www.bioinformatics.com.cn/en>) and g:Profiler (Kolberg et al.,

2023). DEGs without Entrez Gene ID were excluded from the analyses. GO terms were categorized into biological processes (BPs), cellular components (CCs), and molecular functions (MFs). Pathway analysis was also performed using Ingenuity Pathway Analysis (IPA, QIAGEN) software on DEGs that met the criteria of a gene-level fold change < -1.5 or > 1.5 and a false discovery rate (q -value) < 0.05 . DEGs used for the analyses are listed in [Supplementary Table S1](#).

Protein detection by Western blotting

Western blotting was performed as described previously (Brodaczewska et al., 2023). In brief, cells cultured in T25 flasks were detached with Accutase (BioLegend, United States, Cat#423201), washed twice with PBS, and lysed with RIPA buffer containing Cocktail inhibitors (Thermo Fisher Scientific, Waltham, MA, United States; RIPA: Cat#89901 and inhibitors: Cat#78430). Total protein concentration was assessed using the BCA assay (Thermo Fisher Scientific, Cat#23227), and a measure of 20 μ g of total protein solubilized in the Laemmli sample buffer (Thermo Fisher Scientific, Alfa Aesar, Haverhill, MA, United States, Cat#J0015.AC) was loaded on 12% polyacrylamide gel. After transfer onto nitrocellulose membranes (Bio-Rad, Hercules, CA, United States, Cat#1620115), proteins were detected using Ponceau S staining (Thermo Fisher Scientific, Cat#A40000279). Non-specific binding was reduced by blocking (5% skimmed milk, 2 h; room temperature). Membranes were incubated overnight at 4°C in the solution of primary antibodies (anti-MMP1, R&D system, United States, Cat#MAB901), then washed with TBS-Tween, and incubated for 2 h at room temperature with the relevant secondary antibody conjugated with horseradish peroxidase (HRP) (Vector laboratories, United States, anti-Rabbit IgG: Cat#P1-1000, anti-Mouse IgG: Cat#P1-2000). Detection was performed using Luminol as an HRP substrate (Santa-Cruz, CA, United States) with X-ray films. Quantification of the integrated optical density (IOD) of the bands was calculated using ImageJ software and normalized to the IOD of loading control protein–vinculin (Santa-Cruz, CA, United States, Cat #sc-59803).

Detection of secreted factors

Secreted VEGF, pro-MMP1, and total MMP1 were measured from SKOV3 cell culture supernatants after MMC treatment under normoxia and hypoxia using commercially available specific enzyme-linked immunosorbent assay kits (all DuoSet ELISA kits, R&D Systems, United States; VEGF: Cat#DY293B, pro-MMP1: Cat#DY900-05, and total MMP1: Cat#DY901B). Results were normalized to 10^6 cells and calculated from the standard dose-response curve.

Quantitative PCR

Two micrograms of RNA were reverse-transcribed into cDNA using Superscript IV (Thermo Fisher Scientific, Cat#18090050),

according to the manufacturer's protocol, and then subjected to real-time quantitative PCR (RT-qPCR) using Light Cycler 480 (Roche). Amplification conditions were 95°C (5 min), followed by 40 cycles at 95°C (10 s) and 60°C (30 s). The relative abundance of target mRNA was calculated according to the $\Delta\Delta$ cycle threshold method ($\Delta\Delta Ct$). mRNA expression levels of PPIA and GUSB were used as internal controls to normalize each RT-qPCR reaction. The relative expression levels were calculated as fold enrichment of treated cells over control cells. The following TaqMan probes (Thermo Fisher Scientific) were used: MMP1 (Cat#Hs00899658_m1), VEGF (Cat#Hs00900055_m1), PPIA (Cat#Hs01565699_g1), and GUSB (Cat#Hs00939627_m1).

Statistical analysis

Using GraphPad Prism v.10 software (GraphPad Software, San Diego, CA, United States), statistical tests were adjusted for each data set separately. The Shapiro–Wilk test was used to assess the normality of data distribution. For comparison between normoxia and hypoxia control and treated groups, two-way ANOVA followed by a Tukey's *post hoc* test (or Kruskal–Wallis test with Dunn's multiple comparison test for non-Gaussian distribution) was used. Data are expressed as the mean \pm SEM for at least three independent biological experiments ($n \geq 3$) and were considered statistically significant at $p < 0.05$.

Results

Mitomycin C cytotoxicity for SKOV3 cells in normoxia vs. hypoxia

To determine the effect of MMC on SKOV3 cell growth in normoxia and hypoxia, the morphology, cell number, LDH level, Ki67+ population, and cell cycle distribution were examined. [Figures 1A1, A2](#) show cell morphology changes in both pO_2 -values; upon MMC treatment, cells were significantly bigger ($p = 0.0005$ and $p = 0.0007$ in normoxia and hypoxia, respectively) and more granular ($p < 0.0001$). Cell number was significantly reduced by drug treatment in both pO_2 -values ($p < 0.0001$; [Figure 1B](#)), and viability decreased under hypoxia ($p < 0.0001$). MMC was cytotoxic, as indicated by the elevated LDH level reflecting cell membrane damage under both normoxia and hypoxia conditions ($p < 0.0001$; [Figure 1C](#)). The MMC cytotoxic effect was significantly stronger under hypoxia, suggesting potential additive effects of MMC and low pO_2 ($p = 0.02$; [Figure 1C](#)). However, MMC IC_{50} values did not significantly differ substantially upon pO_2 changes ([Supplementary Figure S1A](#)). Exposure to MMC under normoxia ($p = 0.0214$) and hypoxia ($p = 0.0101$; [Figure 1D](#)) increased the Ki67+ cell proportion. [Figure 1E](#) shows the cell cycle distribution. In both pO_2 conditions ($p = 0.0006$ and $p = 0.0007$), MMC reduced the percentage of SKOV3 cells in the G0/G1 phase and induced their accumulation in the S phase ($p = 0.0036$ in normoxia and $p = 0.023$ in hypoxia), similar to the Ki67+ cell distribution (Sun and Kaufman, 2018), without affecting the number of cells in the G2/M phases. Exemplary FACS histograms from cell cycle analysis are shown in [Supplementary Figure S2](#).

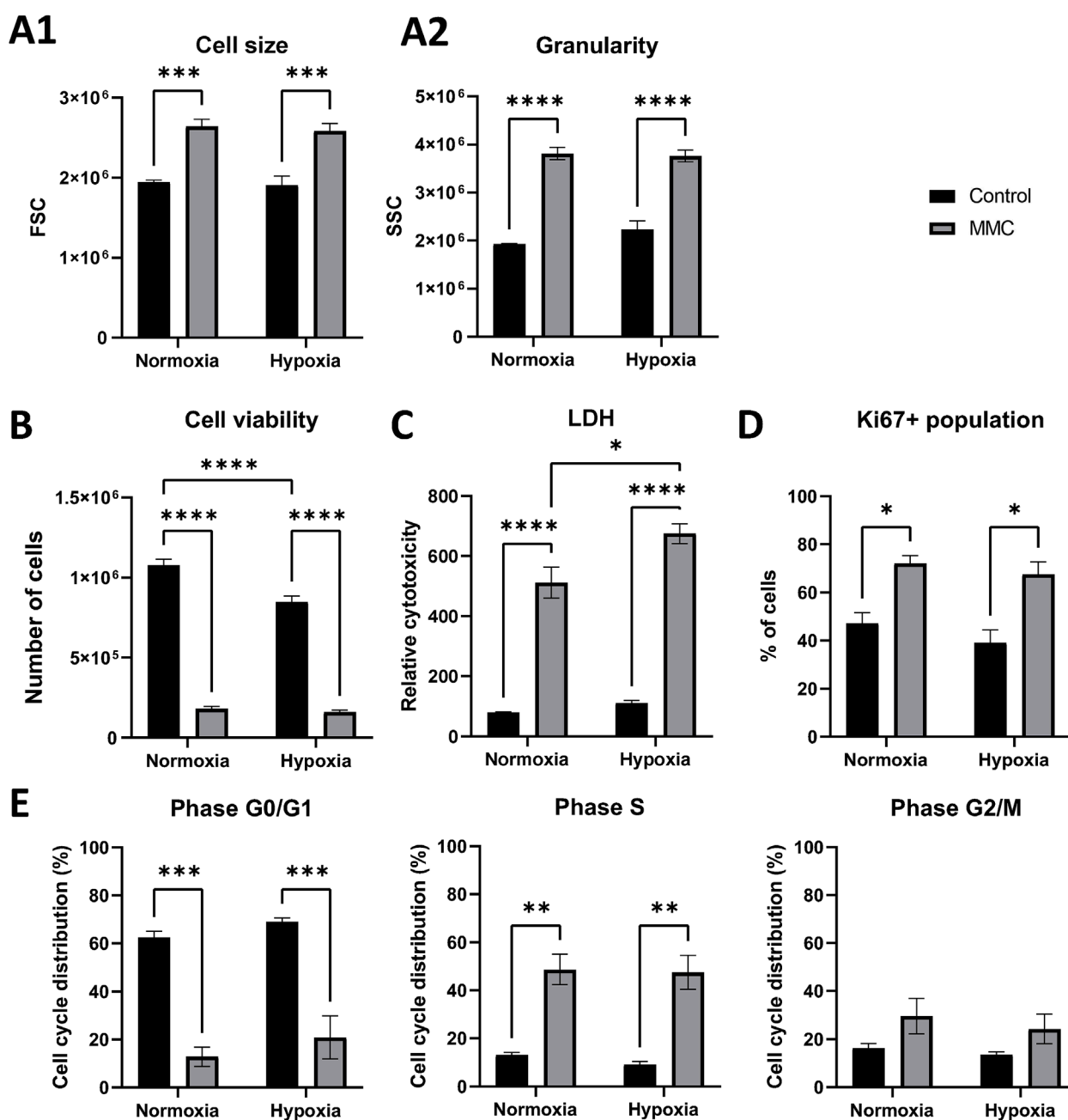


FIGURE 1
Influence of mitomycin C (MMC) on SKOV3 cells under normoxic and hypoxic conditions. (A1) Cell size (FSC) and (A2) granularity (SSC) assessed by flow cytometry. (B) Quantification of number of SKOV3 cells. (C) Relative cytotoxicity of MMC assessed by the LDH assay. (D) Percentage of proliferative Ki67⁺ cells assessed by flow cytometry. (E) The cell cycle studied after propidium iodide (PI) incorporation and flow cytometry assessment: the percentages of cells among G0/G1, S, and G2/M phases of the cell cycle. (A) Detailed statistics description is provided in [Supplementary Table S2](#).

Mitomycin C and hypoxia alter the global gene expression of ovarian cancer cells

As MMC IC₅₀ on SKOV3 cells appeared similar under normoxia and hypoxia, we performed global transcriptome profiling to identify hypoxia-dependent pathways. Gene expression analysis was performed using HTA 2.0, which allows analysis at both the gene and exon levels. PCA analysis of HTA 2.0 data grouped samples into four separate sets, clearly indicating the

proper group segregation ([Figure 2A](#)). PCA1 was responsible for explaining 67.3% of the variance—this dimension separated samples based on MMC treatment. PCA2 explained 25.5% of the variance—this dimension separated samples on the basis of pO₂.

The DEGs were identified: a total of 801 genes were differentially expressed (529 up and 272 down) in hypoxic SKOV3 cells (compared to normoxic cells), 2,985 genes were differentially expressed (1,728 up and 1,257 down) in MMC-treated SKOV3 cells in normoxia

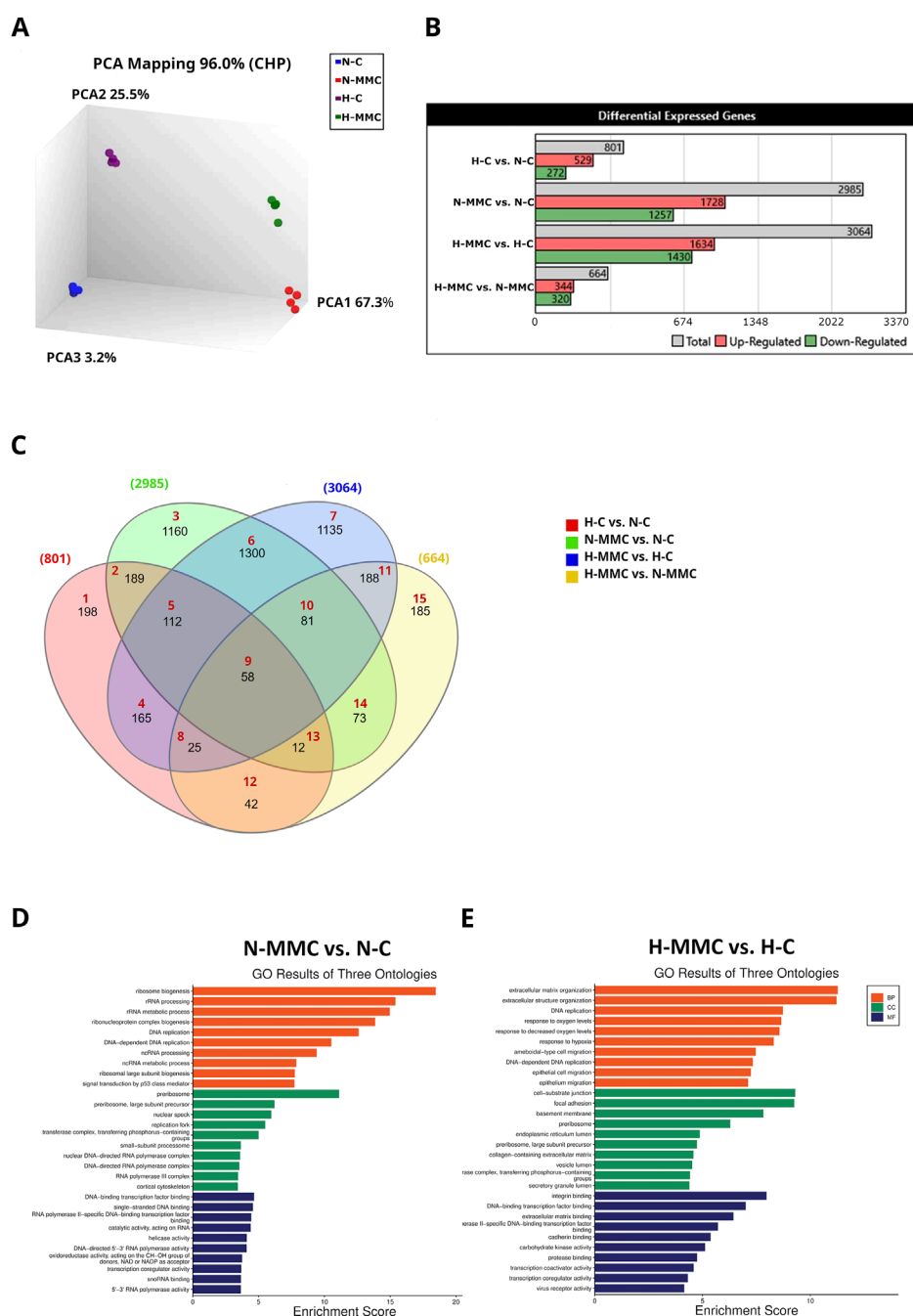


FIGURE 2

Global gene expression in SKOV3 cells treated with mitomycin C (MMC) under normoxia and hypoxia conditions. **(A)** Principal component analysis (PCA). **(B)** Differentially expressed gene analysis in SKOV cells using TAC 4.0.2; fold change < -2 or > 2 ; $p < 0.05$. **(D)** Venn diagram—representing the overlapping groups of transcripts identified in **(B)**, red indicates different groups of genes mentioned in the article, black indicates the number of genes in a given group. $N = 4$. **(D,E)** The most significantly enriched Gene Ontologies (GO) in SKOV3 cells treated with MMC in hypoxia, based on molecular functions (MFs), biological processes (BPs), and cellular components (CCs). The enrichment score was calculated as $-\log(p\text{-value})$. Fold change (FC) ≤ -2 and ≥ 2 ; $p < 0.05$; genes without Entrez Gene ID were excluded from the analysis. Analysis: **(D)** N-MMC vs. N-C. **(E)** H-MMC vs. H-C.

(compared to normoxic control cells), 3,064 genes were differentially expressed (1,634 up and 1,430 down) in MMC-treated hypoxic SKOV3 cells (compared to hypoxic control cells), and 664 genes were differentially regulated (344 up and 320 down) in hypoxic MMC-treated SKOV3 cells (compared to normoxic MMC-treated SKOV3 cells) (Figure 2B). The Venn diagram, in Figure 2C, presents

the numbers of DEGs from all comparisons (H-C vs. N-C, N-MMC vs. N-C, H-MMC vs. H-C, and H-MMC vs. N-MMC). This identifies the commonly expressed (or mutually exclusive) genes for all comparisons. For example, N-C vs. H-C comparison (gene group no. 1, red in the Venn diagram) identifies the genes differently expressed by hypoxic SKOV3 cells, mimicking the natural tumor

environment. The Venn diagram indicates a group of genes modified in SKOV3 cells in both oxygen conditions (no. 6) and genes altered upon MMC treatment, distinctly reacting in normoxia (no. 3) as opposed to hypoxia (no. 7). This also identifies a group of genes (no. 15) that were altered upon MMC treatment but appeared distinguishable only upon comparison of the two pO₂ conditions.

This initial analysis identified candidate genes that are the subject of further research and treatment. Genes modified under all investigated conditions are of particular interest (gene group no. 9); these 58 genes differentially expressed in all comparisons may, therefore, represent potential treatment targets. They are susceptible to MMC, regardless of the pO₂ gradient in the tumor. Other alternatives for therapeutic options are 185 genes from group no. 15, which were differentially modulated between normoxia and hypoxia during MMC treatment, present potential therapeutic agents. These genes a) could not be identified as targets under normoxia conditions because they could only be identified as candidates in hypoxia and b) may represent exclusively effective targets because they are expressed under more physiologically relevant, hypoxic conditions.

Mitomycin C treatment under normoxia affects ribosome biogenesis, whereas under hypoxia, it targets the extracellular matrix, as revealed by GO analysis

GO enrichment pathway analysis (Figure 2D) of DEGs identified in MMC-treated SKOV3 cells in normoxia showed the most significantly affected BPs being connected with ribosome biogenesis (GO:0042254) and rRNA processing (GO:0006364). The most affected CC was the preribosomal component (GO:0030684). The most affected MF was connected with “DNA-binding transcription factors binding” (GO:00140297). When treatment was performed under hypoxia (Figure 2E), the most significantly altered BPs were related to the extracellular matrix and structure organization (GO:0030198 and GO:0043062, respectively), while the most affected CCs concerned cell–substrate junction (GO:0030055) and focal adhesion (GO:0005925). The most affected MFs were related to integrin binding (GO:0005178) and DNA-binding transcription factor binding (GO:00140297). The action of hypoxia was also confirmed by GO analysis (Supplementary Figure S3).

Mitomycin C-induced senescence is impaired by hypoxia

To further differentiate the drug response by normoxic and hypoxic cells, KEGG pathway analysis was performed. It showed that HIF-1 signaling was the most significantly altered pathway in control hypoxic SKOV3 cells (Figure 3A: H-C vs N-C), as confirmed by the upregulation of the VEGF gene and protein expression (H-C vs N-C: mRNA, $p < 0.0001$; secretion, $p = 0.0218$, Figures 4A,B).

Cellular senescence is the most significantly altered process identified by KEGG analysis in normoxic SKOV3 cells after MMC treatment (Figure 3B). When the drug is added under hypoxic conditions, other pathways/processes become more important, including those related to central carbon metabolism in cancer, small-cell lung cancer, glycolysis/gluconeogenesis, HIF-1 signaling,

and focal adhesion (Figure 3C). Moreover, the expression levels of p-S6 and p21 proteins were significantly upregulated upon MMC treatment under normoxia conditions (H-C vs N-C: for p-S6, $p = 0.0323$; for p21, $p = 0.0019$), while under hypoxia conditions, the upregulation was also significant for p21 ($p = 0.0009$) and p-S6 ($p = 0.1627$) (Supplementary Figure S4A–C). Correspondingly, SKOV3 cell size and granularity were significantly increased, suggesting the induction of senescence in response to MMC (Figure 1A1, A2). A total of 22 senescence-related genes were commonly changed in both pO₂-values, while another 12 genes changed only under normoxia (N-MMC vs N-C) and 8 genes only under hypoxia (H-MMC vs. H-C) (listed in Supplementary Figure S5), suggesting that senescence induction involves different pathways depending on pO₂. According to the GO analysis via g:Profiler, the first group is associated with cell division (GO:0051301), and the second group is associated with adenine transport (GO:0015853), indicating that hypoxia significantly modulates the SKOV3 cell response to the drug.

MMP1 is the most upregulated gene from the IL-17 signaling pathway

The KEGG analysis revealed differential effects of pO₂ on MMC-treated SKOV3 cells, highlighting the HIF-1 signaling pathway (hsa04066, Figure 3D), bladder cancer-related processes (hsa05219, Figure 3D), and the IL-17 signaling pathway (hsa04657, Figures 3D,E). *MMP1*, the most upregulated gene in this pathway, changed in all four comparisons, as first shown by the Venn diagram (Figure 2C, gene group no. 8).

MMP1 expression was upregulated under hypoxia ($p < 0.0001$), while MMC treatment reduced *MMP1* under both pO₂ conditions ($p < 0.0001$ in both pO₂). Hypoxia-dependent induction of *MMP1* is abolished by MMC treatment ($p < 0.0001$, Figure 5A). Similar trends in *MMP1* gene expression in hypoxia were observed by RT-qPCR (H-C vs N-C: $p = 0.1250$; H-MMC vs H-C $p = 0.1074$, Figure 5B). *MMP1* protein expression profile, assessed by Western blotting (WB), closely resembled the microarray analysis pattern (H-C vs N-C: $p < 0.0001$; N-MMC vs N-C: $p = 0.0109$; H-MMC vs H-C: $p < 0.0001$; Figures 5C,D). ELISA showed that the secreted pro-*MMP1* (inactive form) significantly increased upon hypoxia ($p = 0.0064$) and tended to be downregulated by MMC ($p = 0.1687$, Figure 5E). Figure 5F shows total secreted *MMP1* (including active and inactive forms of *MMP1*), which was significantly increased by MMC treatment under both normoxia ($p = 0.0047$) and hypoxia ($p = 0.0211$), in contrast to pro-*MMP1*. Pro- and total secreted *MMP1* were also measured in three additional OC cell lines (Supplementary Figure S6), showing variable levels of induction either by MMC or hypoxia. The profiles of expression of the two forms of *MMP1* under the influence of pO₂ and MMC (Supplementary Figure S6) indicate that the four OC cell lines react similarly.

Hypoxia and mitomycin C differentially shape the molecular landscape of genes as revealed by ingenuity pathway analysis

To overview the main biological themes in the transcriptomic data, we performed pathway analysis using IPA software. It

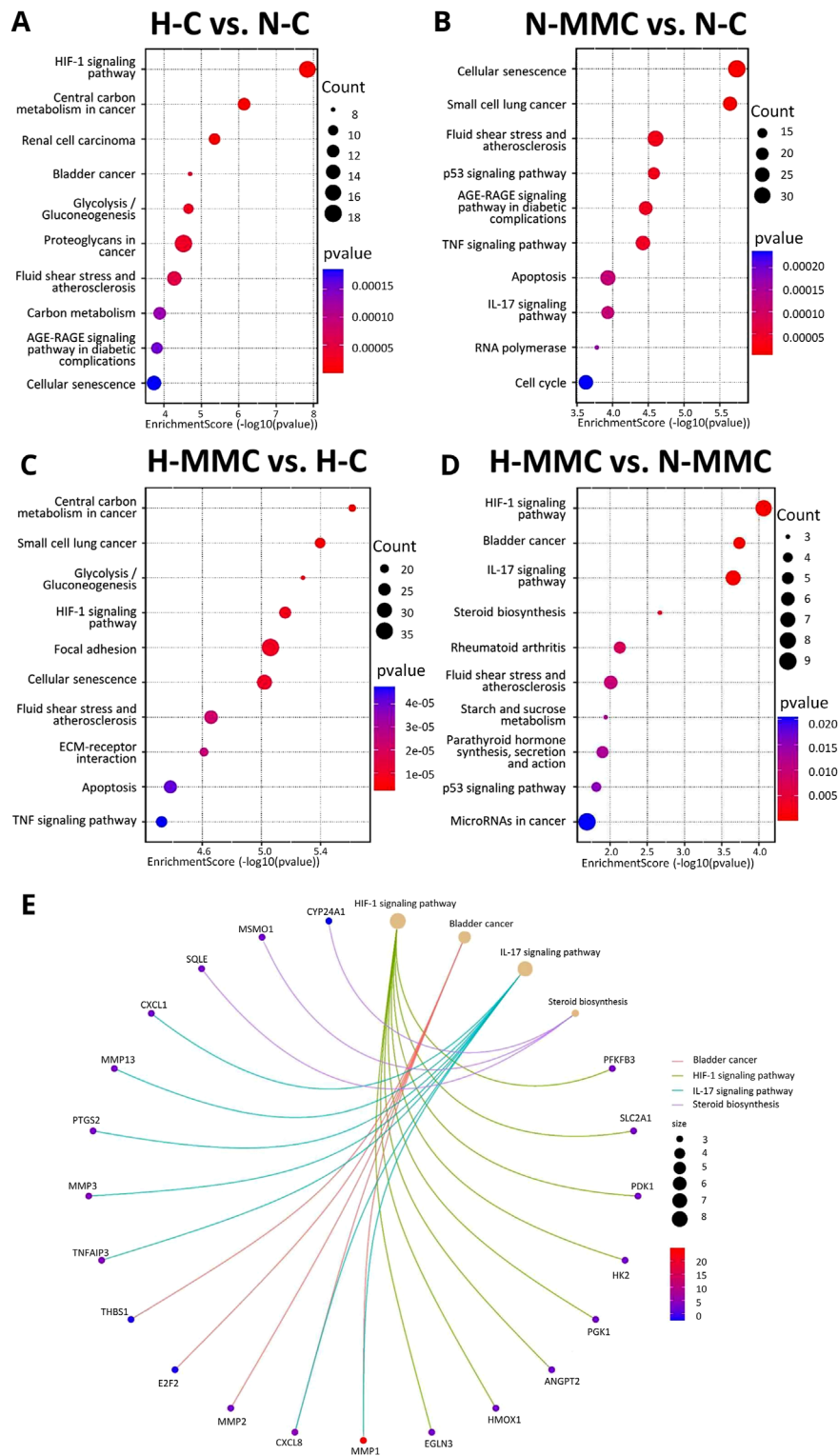


FIGURE 3 Pathways altered in all DEGs identified in SKOV3 cells under the influence of hypoxia and mitomycin C (MMC) based on the KEGG database. **(A)** Effect of hypoxia (H-C vs N-C). **(B)** Effect of MMC in normoxia (N-MMC vs. N-C). **(C)** Effect of MMC in hypoxia (H-MMC vs. H-C). **(D)** Effect of pO₂ on MMC treatment (H-MMC vs. N-MMC). Fold change (FC) ≥ 2 ; $p < 0.05$; genes without Entrez Gene ID were excluded from the analysis. **(E)** C-net plot of pathways/processes altered in SKOV3 cells treated with MMC in hypoxia (vs. N-MMC), based on the KEGG database. Fold change (FC) ≤ -2 and ≥ 2 ; $p < 0.05$; genes without Entrez Gene ID were excluded from the analysis.

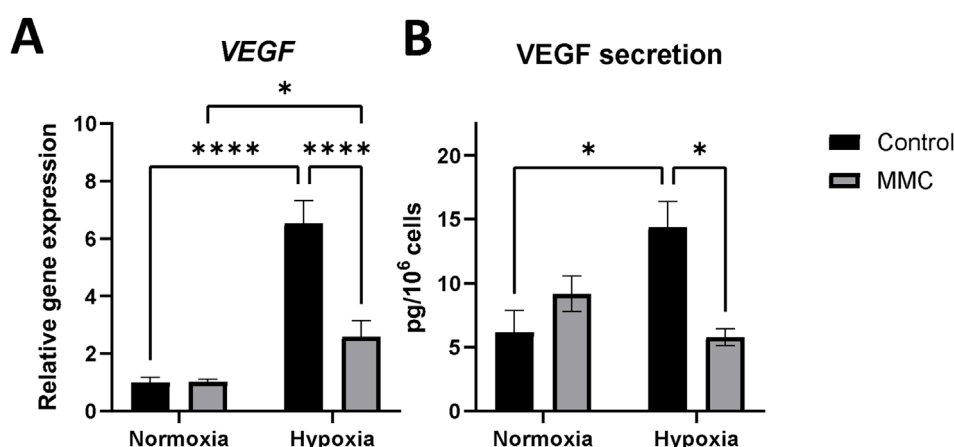


FIGURE 4
Expression of VEGF on gene and protein levels in SKOV3 cells treated with mitomycin C (MMC) in normoxia and hypoxia. **(A)** The *VEGF* mRNA expression level was measured by RT-qPCR and normalized to *PPIA* and *GUSB* expressions and normoxia control as 1. **(B)** Level of VEGF secretion in the cell culture supernatant measured by ELISA; results were normalized to normoxia control set as 1. A detailed statistics description is provided in the [Supplementary Table S2](#).

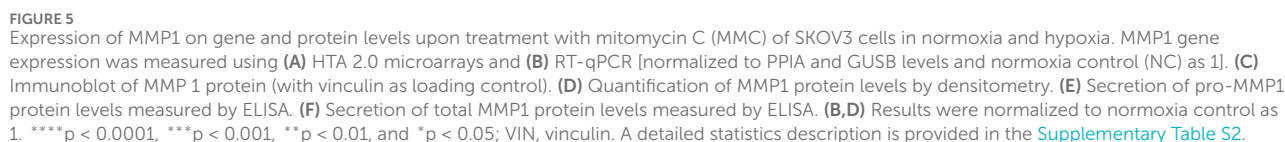
additionally allowed us to identify canonical pathways, upstream regulators, diseases, and biological functions. It also presents their relationships and infers relationships between previously unrelated entities. A graphical summary is shown in [Figure 6](#). The effect of hypoxia ([Figure 6A](#)) was predicted using IPA to be mainly influenced by the activation of *HIF1A*, *VEGFA*, *IL1A*, *IL1B*, *TGFB1*, *F3*, *F10*, *PLCL1*, *PLCL2*, *MMP1*, *EPAS1*, and *EGF* as upstream regulators responsible for the gene expression pattern. The processes predicted to be mostly intensified are related to the development of endothelial cells and vasculature. Hypoxia also accelerates migration and invasion processes. The only genes predicted to be inhibited were *EFNA3* and *EFNA5*. When MMC treatment was performed under normoxic conditions ([Figure 6B](#)), IPA predicted the activation of *VEGFA*, *CD40*, *CCNE1*, *ECSIT*, *E2F1*, *E2F3*, *IFNG*, *IL1A*, *IL1B*, *IL15*, *IL17A*, *TNF*, and *TFDP1*. The processes predicted to be activated were cell cycle-related (S-phase entry and interphase). Other activated processes included tumor growth and cell immortalization. *ACSS2*, *CHCHD5*, *HSPA5* *Mt2*, *MBTPS1*, *NR1H3*, *PNPLA2*, *RLN2*, and *SCAP* were predicted as inhibited. The inhibited pathway was sirtuin signaling. Under hypoxic conditions ([Figure 6C](#)), MMC treatment-activated upstream regulators predicted by IPA were *ACAB*, *CTSS*, *DDIT3*, *HTATIP2*, *IL1A*, *IL1RL2*, *IL18*, *IL24*, *IL32*, *IL36A*, *IRF6*, *MFSD2A*, *NDUFA13*, *NUPR1*, *PYCARD*, *RELA*, and *SOX17*. IPA predicted the inhibition of *ACSS2*, *HIF1A*, *HMOX1*, *HSPA5*, *NR1I2*, *NR1H3*, *PPARG*, *SCAP*, *SDCBP*, *SREBF2*, and *ST8SIA*. IPA predicted enhancement of blood and immune cell death, whereas cell movement and invasion were predicted to be reduced. Hypoxia during MMC treatment ([Figure 6D](#)) resulted in the predicted activation of *EGF*, *FGF2*, *IL1A*, *IL1B*, *IL6*, *IL17A*, *PTGS2*, *TNF*, *SPP1*, and *STAT3*. Among the genes that were predicted by IPA to be activated/inhibited upon MMC treatment, some presented altered transcription within the HTA microarray data ([Supplementary Table S3](#)). The enhanced processes were related to the development of epithelial tissue and endothelial cells, the proliferation of endothelial cells, liver and hepatic stellate

cells, activation of liver cells, angiogenesis in lesions, cell assembly, blood cell adhesion, and an increase in antigen-presenting cells.

To further explore the pO₂ effect on MMC treatment of SKOV3 cells at the intracellular level, we focused on activated and inhibited pathways identified by IPA. The highest z-score (indicating the activation of a given pathway, [Figure 7A](#)) was calculated for pathways related to cholesterol biosynthesis, followed by the negative regulation of rRNA by NoRC and the senescence-associated secretory phenotype (SASP), and methylation-related processes. The most inhibited pathways were RAR-activation and RUNX-regulation of megakaryocyte differentiation and platelet function. Upstream regulator (factors causing the observed gene expression changes) analysis ([Figure 7B](#)) revealed a variety of genes, changing the number of vital cellular and intercellular functions. According to IPA's prediction, the activated regulators were *SPP1*, *MAP2K4*, *IL17F*, *TNC*, *PDGFB*, *LTB4R*, *MIF*, *TGFA*, *IL36A*, *PTGIS*, *CLEC7A*, *US-DDIT3*, *CHD1*, *TRADD*, *MAPK10*, *ILRL2*, *NfκB1-RelA*, and *STAT1/3/5* dimers. *HTATIP2*, *SPNS2*, and *SPRY2* were predicted to be inhibited. The effector genes with increased expression were *PLEC*, *ERRF1*, *SOX9*, *PFKF311*, *NR4A2*, *ITGA2*, *ID2*, *SERPINE*, *RSF*, *CXCR4*, *CXCL2*, *CXCL8*, *CXCL1*, *HMOX1*, *MMP1*, *MMP2*, *IL6ST*, *ANGPT2*, *PKM*, *VEGFA*, *IL6*, *PTGS2*, *HAS2*, *COX HAS2*, *CCL20*, *SLP1*, *LDLR*, *PIRC3*, *IL23A*, *TNFAIP3*, *MMP3*, *MMP13*, *SLC2A1E*, *EDNRA*, and *MMP10*. Downregulated genes included *GNF1B*, *KRT18*, *PALLD*, *COL4A4*, *MDM2*, *CCN2*, *THBS1*, *HIF1A*, *PPARG*, *OCLN*, *COL4A1*, and *VDR*. The predicted activation concerned the development of epithelial and cardiovascular tissues, cell assembly, adhesion of blood cells, migration of phagocytes and myeloid cells, quantity of APCs, tumor angiogenesis, proliferation of hepatic stellate cells, and proteolysis of gelatin.

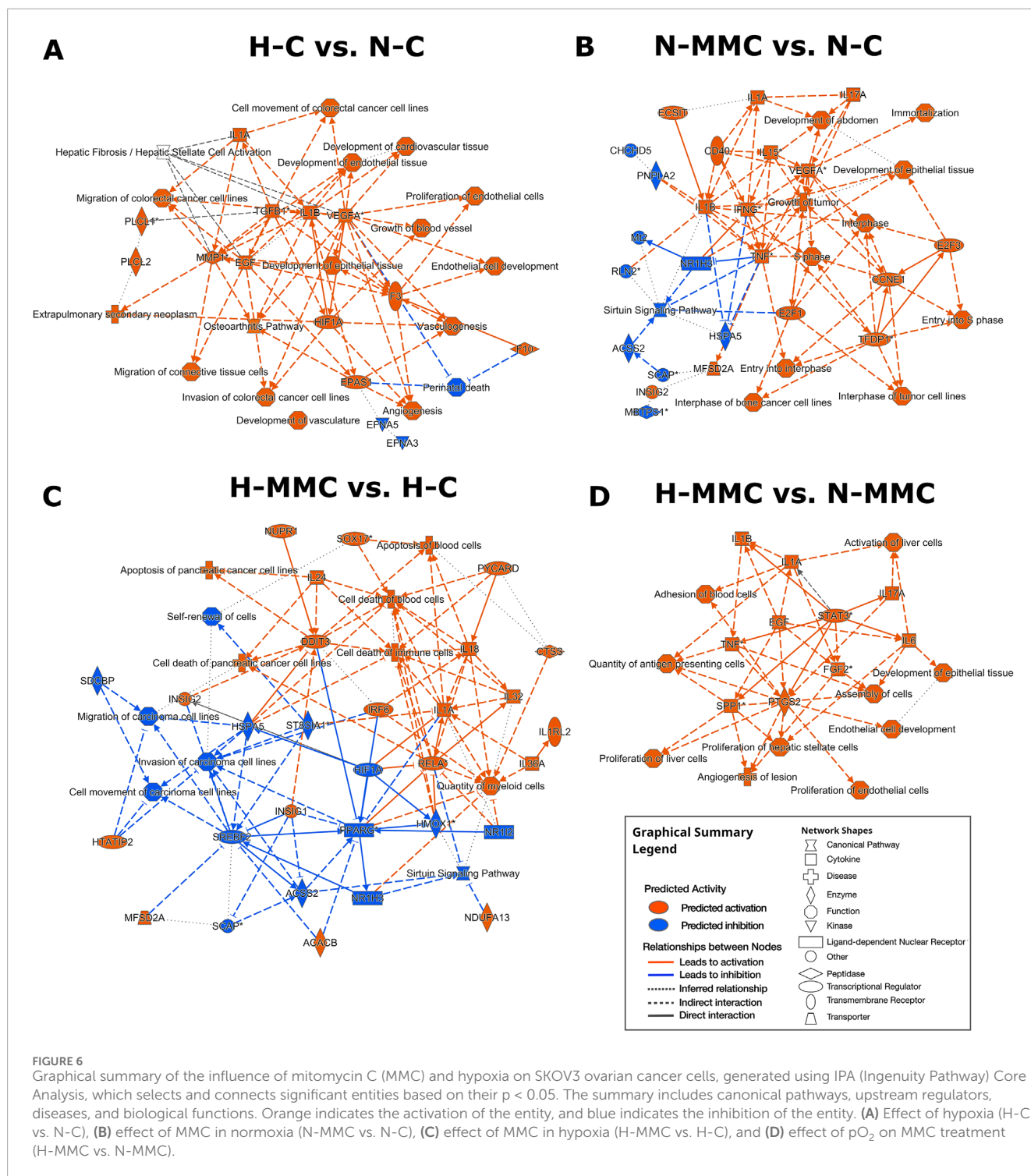
Discussion

To date, the effects of MMC on SKOV3 cells have been studied under standard conditions, i.e., normoxia. We analyzed the



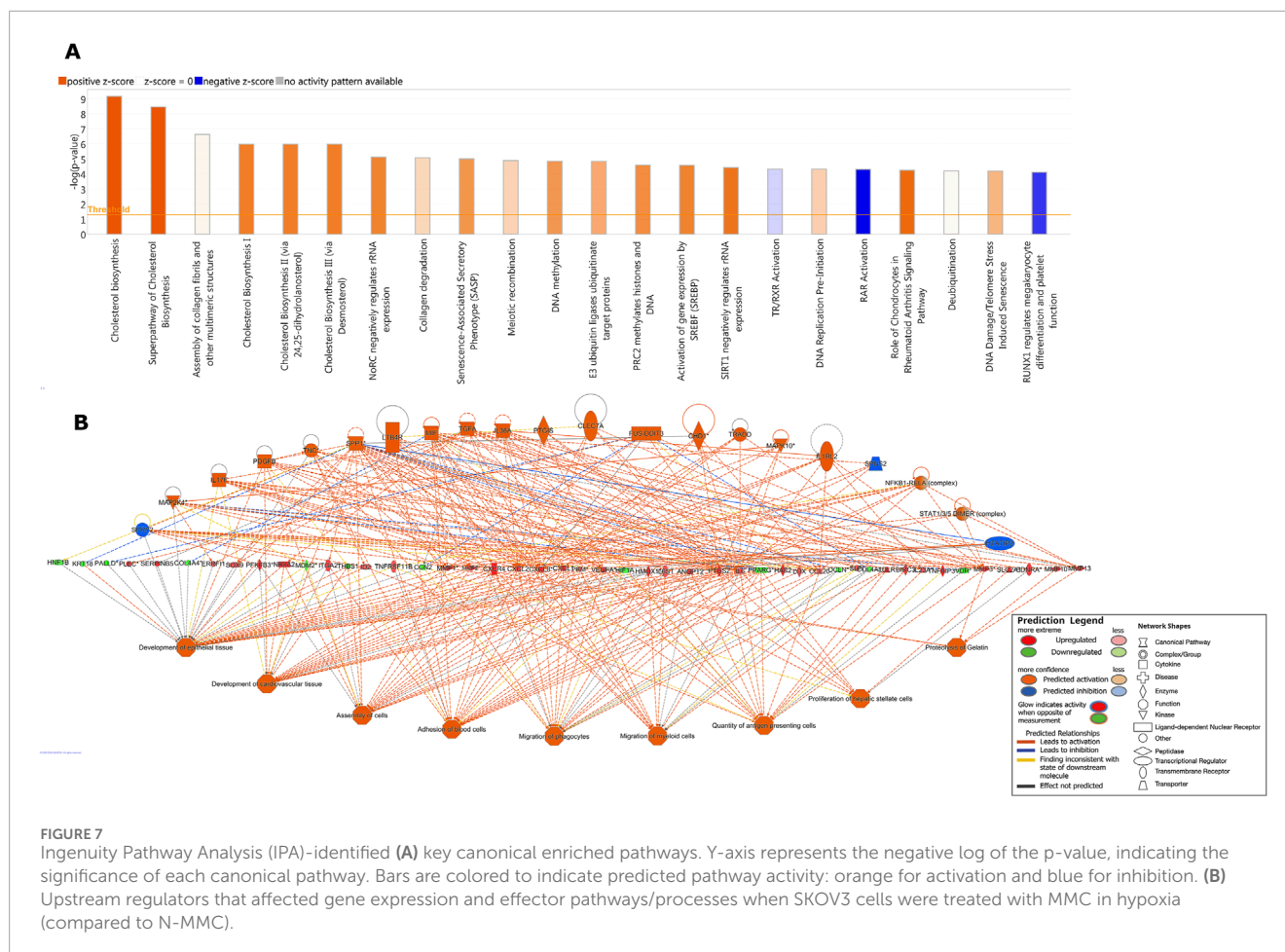
MMC was more cytotoxic toward several types of cells maintained in hypoxia (Teicher and Sartorelli, 1980; Stratford and Stephens, 1989; Mistry et al., 2017). However, in many

To identify the molecular changes due to hypoxia in SKOV3 cells and gain insight into the transcriptomic changes after MMC treatment, we performed analysis using HTA 2.0 microarrays. MMC



was responsible for most of the observed changes in gene expression under both pO_2 conditions. A total of 1,300 differentially expressed transcripts were commonly changed by MMC treatment in both pO_2 -values, but more than 1,000 gene changes were distinct and characteristic for each pO_2 (Figure 2C). GO enrichment pathway analysis revealed that MMC treatment in normoxia affected BPs related to ribosome biogenesis and different types of RNA processing, which is consistent with previous findings on the mechanism of MMC action

(Snodgrass et al., 2010). The preribosome was the most affected CC in normoxia but slightly altered in hypoxia, indicating an influence on protein maturation. Interestingly, hypoxic MMC treatment altered genes related to ECM properties (Figures 2D,E) (Gilkes et al., 2014), which is highly relevant for future translational applications of MMC. GO enrichment analysis also indicated changes upon hypoxic MMC treatment in cell–substrate junction and focal adhesion molecules (Ramteke et al., 2015). Other processes identified by GO



analysis included DNA-binding transcription factor binding. Hypoxia additionally revealed changes in integrin functions, supporting ECM alterations by MMC. Therefore, hypoxia affects the response of OC cells to MMC by involving distinct molecular pathways from normoxia.

ECM-favored mobility and migration of hypoxic cancer cells depend on VEGF, the HIF-1 downstream transcription product and main modulator of angiogenesis. The modulation of VEGF gene expression and protein secretion (Figures 4, Figure 6A), along with the antiangiogenic effects of MMC (Gu et al., 2013; Li et al., 2015), confirms the key effect of pO_2 in determining drug effectiveness.

Moreover, KEGG analysis identified cell senescence as the most significantly altered process in normoxia-MMC treatment, appearing less significant in hypoxia-MMC. MMC treatment affected cell morphology, notably including hallmark features of senescence, as evidenced by increased cell size and granularity (Goy et al., 2023). Different genes being involved under both oxygen conditions indicate distinct pathway activation (cell division in normoxia-MMC vs adenine transport in hypoxia-MMC), leading to the initiation of senescence (Zeng et al., 2018), which is important since senescence escape is favored by hypoxia (Olszewska et al., 2021).

Hypoxia-MMC treatment effects, analyzed by KEGG, revealed the IL-17 signaling pathway (hsa04657) genes in SKOV3 cells. IL17A, elevated in OC, promotes migration and invasion (Bilska et al., 2020; Guo and Zhang, 2022). The predominantly upregulated gene of the IL-17 pathway, *MMP1*, was increased in a HIF1 α -dependent way

(Shin et al., 2015). Checking the intracellular and secreted forms of MMP1, i.e., pro-MMP1, and total MMP1, i.e., MMC, suppressed *MMP1* mRNA expression and blocked its upregulation upon hypoxia (Figure 5). This difference was confirmed at the protein level for MMP1, occurring at the level of secreted proteins; under hypoxia, pro-MMP1 and total secreted form were not suppressed by the drug and even induced by MMC under both conditions. This indicates that the proportions of the active and pro-forms of the enzyme changed. This is important for the potential MMP1 activity in the hypoxic ECM, where it may degrade components like collagen and contribute to metastasis; this was confirmed in other OC cells, where pro- and total MMP1 proteins were upregulated by MMC and hypoxia (Supplementary Figure S6), consistent with previous observations (Shin et al., 2015; Belton et al., 2016; Pal-Ghosh et al., 2019). We report the effects of both factors on MMP1 forms, showing that OC cells may respond to hypoxia (TOV112D), while others were sensitive to MMC (A2780 and ES-2). MMP1 secretion upon hypoxia is redox-dependent (Shin et al., 2015). OC cell lines here (Supplementary Figure S6) show that MMC effects on both forms of the secreted protein are annihilated by hypoxia, proving that although the drug treatment and tumor microenvironment (TME; hypoxia) are activators of MMP1, their action can counteract one another.

Relationships between genes and biological processes uncovered previously unrecognized gene connections and pathways/processes by IPA. When pO_2 was the only difference between MMC treatments

of SKOV3 cells, the IPA canonical pathway analysis revealed strong activation of cholesterol biosynthesis and related pathways (all with z -score >5) (Figure 7A). Cholesterol biosynthesis dysregulation, often observed in OC patients, contributes to disease progression (He et al., 2021; Qusairy et al., 2023). *SPP1*, a gene encoding osteopontin, was among the identified genes recently shown to be important in cholesterol metabolism (Han et al., 2023). *SPP1* levels correlated with clinical parameters and immune response in OC patients (Gao et al., 2022).

Conclusion

Focusing on the data differences between *in vitro* and *in vivo*-like assays results under different TME conditions, this evidences highlights the influence of oxygen availability on cell responses and proves that the lack of consideration of hypoxia as a major regulator leads to data misinterpretation for translational applications.

Investigating the effect of MMC, an antibiotic relatively rarely used in OC therapy, on SKOV3 cells under normoxic and hypoxic conditions changed cell growth, morphology, number, LDH level, Ki67+ population, and cell cycle distribution. MMC- and pO_2 -induced transcriptomic changes were deciphered using HTA 2.0 microarrays. This combined treatment particularly highlighted the effect of pO_2 modification on MMC activity. The most significant data were verified in three other OC cell lines, namely, TOV112D, ES-2, and A2780.

In normoxia, MMC mainly affected several ribosome-related pathways, while it modified the ECM in hypoxia, with *MMP1* as the most significantly upregulated gene and *SPP1* as a fundamental molecular regulator of processes, including cholesterol biosynthesis. Thus, the hypoxia-modified effects of MMC on OC cells uncovered therapeutic target genes to optimize MMC treatment efficacy.

Our data could also contribute to the development of OC cell virtual models that predict cell susceptibility to treatment (Phillips et al., 2000; Molinelli et al., 2013; Kozłowska et al., 2018). Our studies, therefore, open new perspectives in understanding the physiology of OC and will contribute to new models for the development of more effective therapeutic strategies.

Data availability statement

The datasets presented in this study are available at GEO repository, accession number GSE259424 (<https://www.ncbi.nlm.nih.gov/geo/query/acc.cgi?acc=GSE259424>).

Ethics statement

Ethical approval was not required for the studies on humans in accordance with the local legislation and institutional requirements because only commercially available established cell lines were used.

Author contributions

AG: conceptualization, formal analysis, funding acquisition, investigation, methodology, validation, visualization, writing

– original draft, and writing – review and editing. KB: conceptualization, methodology, validation, and writing – review and editing. RI-N: methodology, writing – review and editing, and investigation. MK: data curation, formal analysis, and writing – review and editing. AS: investigation, validation, and writing – review and editing. LB: writing – original draft and writing – review and editing. CS: writing – review and editing. BL: funding acquisition, methodology, resources, and writing – review and editing. RS: conceptualization, funding acquisition, methodology, and writing – review and editing. CK: conceptualization, funding acquisition, methodology, supervision, writing – original draft, and writing – review and editing.

Funding

The author(s) declare that financial support was received for the research and/or publication of this article. The research was funded by the National Science Centre grant no 2012/07/N/NZ5/02052 and subvention of the Ministry of Education and Science, Military Institute of Medicine intramural grant no 1/8912 (412), and partially supported by the University of Warsaw, IDUB action I.3.7.

Conflict of interest

The authors declare that the research was conducted in the absence of any commercial or financial relationships that could be construed as a potential conflict of interest.

The author(s) declared that they were an editorial board member of Frontiers, at the time of submission. This had no impact on the peer review process and the final decision.

Generative AI statement

The author(s) declare that no Generative AI was used in the creation of this manuscript.

Publisher's note

All claims expressed in this article are solely those of the authors and do not necessarily represent those of their affiliated organizations, or those of the publisher, the editors and the reviewers. Any product that may be evaluated in this article, or claim that may be made by its manufacturer, is not guaranteed or endorsed by the publisher.

Supplementary material

The Supplementary Material for this article can be found online at: <https://www.frontiersin.org/articles/10.3389/fcell.2025.1575134/full#supplementary-material>

References

- Bellcross, C. A. (2022). Hereditary breast and ovarian cancer: an updated primer for OB/GYNs. *Obstet. Gynecol. Clin. North Am.* 49 (1), 117–147. doi:10.1016/j.jogc.2021.11.005
- Belton, M., Brilha, S., Manavaki, R., Mauri, F., Nijran, K., Hong, Y. T., et al. (2016). Hypoxia and tissue destruction in pulmonary TB. *Thorax* 71 (12), 1145–1153. doi:10.1136/thoraxjnl-2015-207402
- Bilska, M., Pawlowska, A., Zakrzewska, E., Chudzik, A., Suszczyk, D., Gogacz, M., et al. (2020). Th17 cells and IL-17 as novel immune targets in ovarian cancer therapy. *J. Oncol.* 2020, 8797683. doi:10.1155/2020/8797683
- Bindra, R. S., Gibson, S. L., Meng, A., Westermarck, U., Jasin, M., Pierce, A. J., et al. (2005). Hypoxia-induced down-regulation of BRCA1 expression by E2Fs. *Cancer Res.* 65 (24), 11597–11604. doi:10.1158/0008-5472.CAN-05-2119
- Bogani, G., Matteucci, L., Tamperi, S., Arcangeli, V., Ditto, A., Maltese, G., et al. (2017). The impact of number of cycles of neoadjuvant chemotherapy on survival of patients undergoing interval debulking surgery for stage IIIC-IV unresectable ovarian cancer: results from a multi-institutional study. *Int. J. Gynecol. Cancer* 27 (9), 1856–1862. doi:10.1097/IGC.0000000000001108
- Botrus, G., Roe, D., Jameson, G. S., Junior, P., Korn, R. L., Caldwell, L., et al. (2022). Mitomycin C in homologous recombination deficient metastatic pancreatic cancer after disease progression on platinum-based chemotherapy and olaparib. *Biomedicines* 10 (11), 2705. doi:10.3390/biomedicines10112705
- Bray, F., Laversanne, M., Sung, H., Ferlay, J., Siegel, R. L., Soerjomataram, I., et al. (2024). Global cancer statistics 2022: GLOBOCAN estimates of incidence and mortality worldwide for 36 cancers in 185 countries. *CA Cancer J. Clin.* 74 (3), 229–263. doi:10.3322/caac.21834
- Brodaczewska, K., Majewska, A., Filipiak-Duliban, A., and Kieda, C. (2023). Pten knockout affects drug resistance differently in melanoma and kidney cancer. *Pharmacol. Rep.* 75 (5), 1187–1199. doi:10.1007/s43440-023-00523-y
- Buklaho, P. A., Kisluk, J., and Niklinski, J. (2023). Diagnostics and treatment of ovarian cancer in the era of precision medicine - opportunities and challenges. *Front. Oncol.* 13, 1227657. doi:10.3389/fonc.2023.1227657
- Chen, X., Peng, F., Ji, Y., Xiang, H., Wang, X., Liu, T., et al. (2020). Brca2 deficiency drives gastrointestinal tumor formation and is selectively inhibited by mitomycin C. *Cell Death Dis.* 11 (9), 812. doi:10.1038/s41419-020-03013-8
- Chouaib, S., Umansky, V., and Kieda, C. (2018). The role of hypoxia in shaping the recruitment of proangiogenic and immunosuppressive cells in the tumor microenvironment. *Contemp. Oncol. Pozn.* 22 (1A), 7–13. doi:10.5114/wo.2018.73874
- Collet, G., Skrzypek, K., Grillon, C., Matejuk, A., El Hafni-Rahbi, B., Lamerant-Fayel, N., et al. (2012). Hypoxia control to normalize pathologic angiogenesis: potential role for endothelial precursor cells and miRNAs regulation. *Vasc. Pharmacol.* 56 (5–6), 252–261. doi:10.1016/j.vph.2012.03.001
- Colombo, N., Sessa, C., du Bois, A., Ledermann, J., McCluggage, W. G., McNeish, I., et al. (2019). ESMO-ESGO consensus conference recommendations on ovarian cancer: pathology and molecular biology, early and advanced stages, borderline tumours and recurrent disease†. *Ann. Oncol.* 30 (5), 672–705. doi:10.1093/annonc/mdz062
- Duan, Y., Zhang, P., Zhang, T., Zhou, L., and Yin, R. (2023). Characterization of global research trends and prospects on platinum-resistant ovarian cancer: a bibliometric analysis. *Front. Oncol.* 13, 1151871. doi:10.3389/fonc.2023.1151871
- Evans, C. E., Branco-Price, C., and Johnson, R. S. (2012). HIF-mediated endothelial response during cancer progression. *Int. J. Hematol.* 95 (5), 471–477. doi:10.1007/s12185-012-1072-3
- Fanale, D., Bazan, V., Caruso, S., Castiglia, M., Bronte, G., Rolfo, C., et al. (2013). Hypoxia and human genome stability: downregulation of BRCA2 expression in breast cancer cell lines. *Biomed. Res. Int.* 2013, 746858. doi:10.1155/2013/746858
- Gao, W., Liu, D., Sun, H., Shao, Z., Shi, P., Li, T., et al. (2022). SPP1 is a prognostic related biomarker and correlated with tumor-infiltrating immune cells in ovarian cancer. *BMC Cancer* 22 (1), 1367. doi:10.1186/s12885-022-10485-8
- Gilkes, D. M., Semenza, G. L., and Wirtz, D. (2014). Hypoxia and the extracellular matrix: drivers of tumour metastasis. *Nat. Rev. Cancer* 14 (6), 430–439. doi:10.1038/nrc3726
- Gorodnova, T. V., Kotiv, K. B., Ivantsov, A. O., Mikheyeva, O. N., Mikhailiuk, G. I., Lisyanskaya, A. S., et al. (2018). Efficacy of neoadjuvant therapy with cisplatin plus mitomycin C in BRCA1-mutated ovarian cancer. *Int. J. Gynecol. Cancer* 28 (8), 1498–1506. doi:10.1097/IGC.0000000000001352
- Gorodnova, T. V., Sokolenko, A. P., Kondratiev, S. V., Kotiv, K. B., Belyaev, A. M., Berlev, I. V., et al. (2020). Mitomycin C plus cisplatin for systemic treatment of recurrent BRCA1-associated ovarian cancer. *Invest New Drugs* 38 (6), 1872–1878. doi:10.1007/s10637-020-00965-8
- Gorodnova, T. V., Sokolenko, A. P., Kotiv, K. B., Sokolova, T. N., Ivantsov, A. O., Guseynov, K. D., et al. (2021). Neoadjuvant therapy of BRCA1-driven ovarian cancer by combination of cisplatin, mitomycin C and doxorubicin. *Hered. Cancer Clin. Pract.* 19 (1), 14. doi:10.1186/s13053-021-00173-2
- Goy, E., Martin, N., Drullion, C., Saas, L., Molendi-Coste, O., Pineau, L., et al. (2023). Flow cytometry-based method for efficient sorting of senescent cells. *Bio Protoc.* 13 (7), e4612. doi:10.21769/BioProtoc.4612
- Gu, F., Li, X., Kong, J., Pan, B., Sun, M., Zheng, L., et al. (2013). VEGF111b, a new member of VEGFxxx isoforms and induced by mitomycin C, inhibits angiogenesis. *Biochem. Biophys. Res. Commun.* 441 (1), 18–24. doi:10.1016/j.bbrc.2013.09.144
- Guo, N., and Zhang, J. (2022). Interleukin-17 promotes the development of ovarian cancer through upregulation of MTA1 expression. *Am. J. Cancer Res.* 12 (12), 5646–5656.
- Han, H., Ge, X., Komakula, S. S. B., Desert, R., Das, S., Song, Z., et al. (2023). Macrophage-derived osteopontin (SPP1) protects from nonalcoholic steatohepatitis. *Gastroenterology* 165 (1), 201–217. doi:10.1053/j.gastro.2023.03.228
- He, J., Siu, M. K. Y., Ngan, H. Y. S., and Chan, K. K. L. (2021). Aberrant cholesterol metabolism in ovarian cancer: identification of novel therapeutic targets. *Front. Oncol.* 11, 738177. doi:10.3389/fonc.2021.738177
- Heberle, H., Meirelles, G. V., da Silva, F. R., Telles, G. P., and Minghim, R. (2015). InteractiVenn: a web-based tool for the analysis of sets through Venn diagrams. *BMC Bioinformatics* 16, 169–263. doi:10.1186/s12859-015-0611-3
- Hoskins, P. J., McMurtrie, E., and Swenerton, K. D. (1990). A phase II trial of mitomycin in patients with epithelial ovarian carcinoma resistant to cisplatin or carboplatin. *Am. J. Clin. Oncol.* 13 (5), 416–419. doi:10.1097/00000421-199010000-00010
- Klemba, A., Bodnar, L., Was, H., Brodaczewska, K. K., Wcislo, G., Szczylk, C. A., et al. (2020). Hypoxia-Mediated decrease of ovarian cancer cells reaction to treatment: significance for chemo- and immunotherapies. *Int. J. Mol. Sci.* 21 (24), 9492. doi:10.3390/ijms21249492
- Koczan, D., Fitzner, B., Zettl, U. K., and Hecker, M. (2018). Microarray data of transcriptome shifts in blood cell subsets during S1P receptor modulator therapy. *Sci. Data* 5, 180145. doi:10.1038/sdata.2018.145
- Kolberg, L., Raudvere, U., Kuzmin, I., Adler, P., Vilo, J., and Peterson, H. (2023). g:Profiler—interoperable web service for functional enrichment analysis and gene identifier mapping (2023 update). *Nucleic Acids Research.* doi:10.1093/nar/gkad347
- Kozłowska, E., Farkkila, A., Vallius, T., Carpen, O., Kempainen, J., Grenman, S., et al. (2018). Mathematical modeling predicts response to chemotherapy and drug combinations in ovarian cancer. *Cancer Res.* 78 (14), 4036–4044. doi:10.1158/0008-5472.CAN-17-3746
- Li, A. G., Murphy, E. C., Culhane, A. C., Powell, E., Wang, H., Bronson, R. T., et al. (2018). BRCA1-IRIS promotes human tumor progression through PTEN blockade and HIF-1α activation. *Proc. Natl. Acad. Sci. U. S. A.* 115 (41), E9600–E9609. doi:10.1073/pnas.1807112115
- Li, X., Gu, F., Niu, C., Wang, Y., Liu, Z., Li, N., et al. (2015). VEGF111b, a C-terminal splice variant of VEGF-A and induced by mitomycin C, inhibits ovarian cancer growth. *J. Transl. Med.* 13, 164. doi:10.1186/s12967-015-0522-0
- Lister-Sharp, D., McDonagh, M. S., Khan, K. S., and Kleijnen, J. (2000). A rapid and systematic review of the effectiveness and cost-effectiveness of the taxanes used in the treatment of advanced breast and ovarian cancer. *Health Technol. Assess.* 4 (17), 1–113. doi:10.3310/hta4170
- Lu, Y., Chu, A., Turker, M. S., and Glazer, P. M. (2011). Hypoxia-induced epigenetic regulation and silencing of the BRCA1 promoter. *Mol. Cell Biol.* 31 (16), 3339–3350. doi:10.1128/MCB.01121-10
- Mistry, I. N., Thomas, M., Calder, E. D. D., Conway, S. J., and Hammond, E. M. (2017). Clinical advances of hypoxia-activated prodrugs in combination with radiation therapy. *Int. J. Radiat. Oncol. Biol. Phys.* 98 (5), 1183–1196. doi:10.1016/j.ijrobp.2017.03.024
- Molinelli, E. J., Korkut, A., Wang, W., Miller, M. L., Gauthier, N. P., Jing, X., et al. (2013). Perturbation biology: inferring signaling networks in cellular systems. *PLoS Comput. Biol.* 9 (12), e1003290. doi:10.1371/journal.pcbi.1003290
- Olszewska, A., Borkowska, A., Granica, M., Karolczak, J., Zglinicki, B., Kieda, C., et al. (2021). Escape from cisplatin-induced senescence of hypoxic lung cancer cells can be overcome by hydroxychloroquine. *Front. Oncol.* 11, 738385. doi:10.3389/fonc.2021.738385
- Pal-Ghosh, S., Tadvalkar, G., Lieberman, V. R., Guo, X., Zieske, J. D., Hutcheon, A., et al. (2019). Transient Mitomycin C-treatment of human corneal epithelial cells and fibroblasts alters cell migration, cytokine secretion, and matrix accumulation. *Sci. Rep.* 9 (1), 13905. doi:10.1038/s41598-019-50307-9
- Phillips, R. M., Burger, A. M., Loadman, P. M., Jarrett, C. M., Swaine, D. J., and Fiebig, H. H. (2000). Predicting tumor responses to mitomycin C on the basis of DT-diaphorase activity or drug metabolism by tumor homogenates: implications for enzyme-directed bio-reductive drug development. *Cancer Res.* 60 (22), 6384–6390.

- Pignata, S., Pisano, C., Di Napoli, M., Cecere, S. C., Tambaro, R., and Attademo, L. (2019). Treatment of recurrent epithelial ovarian cancer. *Cancer* 125 (Suppl. 24), 4609–4615. doi:10.1002/cncr.32500
- Qusairy, Z., Gangloff, A., and Leung, S. O. A. (2023). Dysregulation of cholesterol homeostasis in ovarian cancer. *Curr. Oncol.* 30 (9), 8386–8400. doi:10.3390/curroncol30090609
- Ramteke, A., Ting, H., Agarwal, C., Mateen, S., Somasagara, R., Hussain, A., et al. (2015). Exosomes secreted under hypoxia enhance invasiveness and stemness of prostate cancer cells by targeting adherens junction molecules. *Mol. Carcinog.* 54 (7), 554–565. doi:10.1002/mc.22124
- Shih, H. J., Chang, H. F., Chen, C. L., and Torng, P. L. (2021). Differential expression of hypoxia-inducible factors related to the invasiveness of epithelial ovarian cancer. *Sci. Rep.* 11 (1), 22925. doi:10.1038/s41598-021-02400-1
- Shin, D. H., Dier, U., Melendez, J. A., and Hempel, N. (2015). Regulation of MMP-1 expression in response to hypoxia is dependent on the intracellular redox status of metastatic bladder cancer cells. *Biochim. Biophys. Acta* 1852 (12), 2593–2602. doi:10.1016/j.bbadis.2015.09.001
- Snodgrass, R. G., Collier, A. C., Coon, A. E., and Pritsos, C. A. (2010). Mitomycin C inhibits ribosomal RNA: a novel cytotoxic mechanism for bioreductive drugs. *J. Biol. Chem.* 285 (25), 19068–19075. doi:10.1074/jbc.M109.040477
- Stec, R., Bodnar, L., Smoter, M., Korniluk, J., Kuchar, A., Mlot, B., et al. (2014). Mitomycin C and high-dose 5-fluorouracil with folinic acid as a therapeutic option for heavily pretreated patients with metastatic colorectal cancer: prospective phase II trial. *Oncologist* 19 (4), 356–357. doi:10.1634/theoncologist.2014-0029
- Stratford, I. J., and Stephens, M. A. (1989). The differential hypoxic cytotoxicity of bioreductive agents determined *in vitro* by the MTT assay. *Int. J. Radiat. Oncol. Biol. Phys.* 16 (4), 973–976. doi:10.1016/0360-3016(89)90898-5
- Strese, S., Fryknas, M., Larsson, R., and Gullbo, J. (2013). Effects of hypoxia on human cancer cell line chemosensitivity. *BMC Cancer* 13, 331. doi:10.1186/1471-2407-13-331
- Sun, X., and Kaufman, P. D. (2018). Ki-67: more than a proliferation marker. *Chromosoma* 127 (2), 175–186. doi:10.1007/s00412-018-0659-8
- Sung, H., Ferlay, J., Siegel, R. L., Laversanne, M., Soerjomataram, I., Jemal, A., et al. (2021). Global cancer statistics 2020: GLOBOCAN estimates of incidence and mortality worldwide for 36 cancers in 185 countries. *CA Cancer J. Clin.* 71 (3), 209–249. doi:10.3322/caac.21660
- Sznurkowski, J. J. (2023). To bev or not to bev during ovarian cancer maintenance therapy? *Cancers (Basel)* 15 (11), 2980. doi:10.3390/cancers15112980
- Teicher, B. A., and Sartorelli, A. C. (1980). Nitrobenzyl halides and carbamates as prototype bioreductive alkylating agents. *J. Med. Chem.* 23 (8), 955–960. doi:10.1021/jm00182a027
- Villalona-Calero, M. A., Duan, W., Zhao, W., Shilo, K., Schaaf, L. J., Thurmond, J., et al. (2016). Veliparib alone or in combination with mitomycin C in patients with solid tumors with functional deficiency in homologous recombination repair. *J. Natl. Cancer Inst.* 108 (7), djv437. doi:10.1093/jnci/djv437
- Zeng, S., Shen, W. H., and Liu, L. (2018). Senescence and cancer. *Cancer Transl. Med.* 4 (3), 70–74. doi:10.4103/ctm.ctm_22_18